














RESEARCH ARTICLE

The role of the amygdala in ictal central apnea: insights from brain MRI morphometry

Elisa Micalizzi^{1,2} , Alice Ballerini² , Giada Giovannini² , Maria Cristina Cioclu² ,
Simona Scolastico² , Matteo Pugnaghi² , Niccolò Orlandi² , Marcella Malagoli³ ,
Maurilio Genovese³ , Alessandra Todeschini³, Leandra Giunta² , Flavio Villani¹ ,
Stefano Meletti²  & Anna Elisabetta Vaudano² 

¹Department of Neuroscience, IRCCS San Martino Hospital, Genoa, Italy

²Department of Biomedical, Metabolic and Neural Sciences, University of Modena and Reggio Emilia, Modena, Italy

³Department of Radiology, AOU Modena, Modena, Italy

Correspondence

Stefano Meletti, Ospedale Civile Baggiovara (OCB), Azienda Ospedaliero Universitaria of Modena, Via Giardini 1355, Modena 41100, Italy. E-mail: stefano.meletti@unimore.it

Funding information

This study was supported by a grant "Dipartimenti di eccellenza 2018–2022," MIUR, Italy, to the Department of Biomedical, Metabolic and Neural Sciences and by a grant "Ricerca Finalizzata," project code NET-2013-02355313, Ministry of Health to the Azienda Ospedaliero-Universitaria di Modena "Centro hub chirurgia epilessia" (DGR 1172/18).

Received: 22 June 2023; Revised: 9 October 2023; Accepted: 23 October 2023

Annals of Clinical and Translational Neurology 2024; 11(1): 121–132

doi: 10.1002/acn3.51938

Abstract

Objective: Ictal central apnea (ICA) is a frequent correlate of focal seizures, particularly in temporal lobe epilepsy (TLE), and regarded as a potential electroclinical biomarker of sudden unexpected death in epilepsy (SUDEP). Aims of this study are to investigate morphometric changes of subcortical structures in ICA patients and to find neuroimaging biomarkers of ICA in patients with focal epilepsy. **Methods:** We prospectively recruited focal epilepsy patients with recorded seizures during a video-EEG long-term monitoring with cardiorespiratory polygraphic recordings from April 2020 to September 2022. Participants were accordingly subdivided into two groups: patients with focal seizures with ICA (ICA) and without (noICA). A pool of 30 controls matched by age and sex was collected. All the participants underwent MRI scans with volumetric high-resolution T1-weighted images. Post-processing analyses included a whole-brain VBM analysis and segmentation algorithms performed with FreeSurfer. **Results:** Forty-six patients were recruited (aged 15–60 years): 16 ICA and 30 noICA. The whole-brain VBM analysis showed an increased gray matter volume of the amygdala ipsilateral to the epileptogenic zone (EZ) in the ICA group compared to the noICA patients. Amygdala sub-segmentation analysis revealed an increased volume of the whole amygdala, ipsilateral to the EZ compared to controls [$F(1, 76) = 5.383$, $pFDR = 0.042$] and to noICA patients [$F(1, 76) = 5.383$, $pFDR = 0.038$], specifically of the basolateral complex (respectively $F(1, 76) = 6.160$, $pFDR = 0.037$; $F(1, 76) = 5.121$, $pFDR = 0.034$). **Interpretation:** Our findings, while confirming the key role of the amygdala in participating in ictal respiratory modifications, suggest that structural modifications of the amygdala and its subnuclei may be valuable morphological biomarkers of ICA.

Introduction

Ictal central apnea (ICA) is a frequent clinical correlate of focal seizures, being observed in 40–43% of patients with focal epilepsy admitted to Epilepsy Monitoring Units (EMUs).^{1,2} ICA is regarded as a potential electroclinical biomarker of sudden unexpected death in epilepsy (SUDEP), as ictal respiratory disruption has been demonstrated to be a relevant mechanism leading to a fatal outcome.^{2,3}

Recent evidence supports ICA as a distinctive ictal semiological feature of TLE, in particular as a hint of the limbic network involvement.^{1,2,4,5} Data suggesting a functional connection between the amygdala and the neural respiratory networks in the brainstem derive from experimental studies conducted on animals.^{6–9} In humans, evidence of the relevance of the limbic network in the respiratory network can be found in electroclinical and invasive neurophysiological studies carried out for

surgical purposes.^{8,10} More recently, researchers' attention has focused on the role of the amygdala in generating the seizure-related central apneic response.^{11–14} As demonstrated by studies that utilized stereo-EEG combined with video-EEG and cardiorespiratory polygraphy, both the primary and secondary involvement of the amygdala, especially of the basolateral complex, throughout the epileptic discharge, were strongly associated with ICA.^{12–14}

Although ictal respiratory modifications are considered to be associated with a higher risk of SUDEP, data regarding morphometric modifications of subcortical structures in relation to ICA occurrence are scarce. Herein, we aim to investigate subtle morphometric changes of subcortical structures in ICA patients, specifically of the amygdala, thalamic, and brainstem subnuclei, and to find valuable neuroimaging biomarkers of ICA in patients with focal epilepsy.

Materials and Methods

Study population

Patients were prospectively recruited among patients with epilepsy admitted to the EMU at the Ospedale Civile of Baggiovara, Modena Academic Hospital (Modena, Italy) from April 2020 to September 2022.

Each patient underwent a video-EEG long-term monitoring (VLTM) with a 10–20 EEG system (Nihon Kohden Neurofax EEG-1200, Mod JE-120) integrated with a standard precordial single-channel electrocardiogram (EKG), pulse-oximetry for SpO₂ measurement, and a thoracoabdominal belt for respiratory inductance plethysmography. Patients were included according to the following criteria: (i) age over 14 at the time of hospitalization; (ii) having a diagnosis of focal epilepsy; (iii) having at least one focal seizure recorded during VLTM with cardiorespiratory polygraphy (EKG, pulse-oximetry and thoracoabdominal respiratory inductance plethysmography); (iv) having performed a high-resolution 3D T1-weighted brain MRI scan; (v) normal appearance of amygdala structures at visual MRI inspection by expert neuroradiologists. Patients were excluded if (i) they had a large brain lesion involving the subcortical structures and/or underwent neurosurgical procedures; (ii) poor quality of MRI scans.

According to published criteria,^{1,2,4,5,15} apnea was considered as a respiratory arrest of 5 or more seconds visible on the pneumographic channel, preceded and followed by stable breathing for at least 5 sec, and confirmed by visual inspection of the recorded video.

For each patient, the following electroclinical data were collected: age at the time of admission, sex, age at 3D-T1-weighted brain MRI, age of epilepsy onset, disease duration, lobe and hemisphere of the epileptogenic zone (EZ),

family history of epilepsy, febrile seizures in past medical history, number of antiseizure medications (ASMs) at the time of brain MRI, ASMs response according to ILAE definition of drug-resistance.¹⁶ As regards the ICA patients, further electroclinical information was collected: apnea duration, hypoxemia duration, and nadir.

Patients were then classified into TLE and extra-TLE (frontal, insular, occipital and parietal lobe epilepsy) according to an anatomico-electroclinical criterion based on each patient's recorded seizures.

Patients meeting the inclusion criteria were subdivided into two groups: ICA and noICA patients in relation to ICA occurrence during the VLTM. A further analysis was performed considering only the patients with TLE subdivided in ICA-TLE and noICA-TLE. A pool of 30 controls matched by age and sex was collected.

Magnetic resonance imaging (MRI) acquisition

All the included patients and controls underwent a 3T brain MRI for clinical purposes, adopting an epilepsy-dedicated standardized protocol which included a 3DT1-weighted volumetric image (3D-T1W).^{17,18} MRIs were performed on a 3T scanner (3.0 Tesla GE Healthcare, Chicago, USA). Each patient was interviewed before the MRI scan to check for seizures occurring in the 48 h before the exam and no patient reported seizures in this time window. Patients with an increased signal on T2 or FLAIR-weighted images of the amygdala were excluded from the subsequent analysis. Controls underwent a structural MRI scan on the same scanner and with the identical protocol of patients. Quality check (QC) on images was twofold: (i) a qualitative QC considering the main common artifacts, including motion, ringing, and susceptibility. This visual-performed quality check ended with the judgment of “pass” for images with good quality or “fail” otherwise, following previous published workflow¹⁹; (ii) a quality assurance process (outlier detection based on interquartile of 1.5 SDs along with visual inspection of segmentations), was performed adopting a standardized ENIGMA (<http://enigma.usc.edu>), protocols as implemented in previous large-scale case-control studies of epilepsy.^{20–22}

MRI post-processing

Voxel-based morphometry

For the voxel-based morphometry (VBM) analysis, 3D-T1W images were utilized. Preprocessing and statistical analysis were performed using the computational anatomy toolbox (CAT12) and SPM12 (Statistical Parametric Mapping; <http://www.fil.ion.ucl.ac.uk/spm>) on Matlab

2020b (MathWorks, USA). First, the original NIfTI files were flipped to account for the side of the epileptic focus using SPM12. The X-axis was turned negative for all the right-sided patients in order to have the epileptic hemisphere on the left side for all the patients enrolled. Next, the scans were normalized according to the Montreal Neurological Institute (MNI) template using the high-dimensional DARTEL algorithm and modulated by multiplying the Jacobian determinant for each voxel in SPM12. Images were segmented into GM, WM, and cerebrospinal fluid (CSF) in CAT12, and finally, the resulted GM images were smoothed using 8-mm full-width-half-maximum Gaussian smoothing in SPM12. To search for subcortical volume differences across groups, two-sample *t*-tests ($P < 0.001$, minimum threshold cluster of 30 voxels) were performed in SPM12 between ICA versus noICA, ICA versus controls, and noICA versus controls. The same statistical analyses were carried out for the TLE subgroups (i.e., ICA-TLE, noICA-TLE, and controls).

Surface-based morphometry

The 3D-T1W images were analyzed using a standardized image toolbox (FreeSurfer, v7.1, <https://surfer.nmr.mgh.harvard.edu>). Furthermore, the amygdala, hippocampus, thalamus, and brainstem were parcellated using FreeSurfer dev version (<ftp://surfer.nmr.mgh.harvard.edu/pub/dist/freesurfer/dev>) according to their respective pipelines.^{23–26} Specifically, for the amygdala, the extracted nuclei were the anterior amygdaloid area (AAA), cortico-amygdaloid transition area (CAT), and the basal (Ba), lateral (La), accessory basal (AB), central (Ce), cortical (Co), medial (Me), and paralaminar (PL) nuclei (Figure S1A). These nuclei were also clustered in three major complexes adopting the pipeline already published by our group²⁷: (i) the basolateral amygdala (BLA), who included the basal, lateral, accessory-basal, and paralaminar nuclei; (ii) the central-medial complex (CMC), composed by the central and the medial nuclei; (iii) the cortical complex (CO), who included just the cortical nucleus. The AAA and the CAT were considered “other nuclei.”

For the hippocampus, the following subfields were obtained: CA1, CA3, CA4, subiculum, presubiculum, parasubiculum, the molecular and granule cell layers of the dentate gyrus (GCMLDG), the molecular layer, hippocampal tail, and the hippocampal amygdala transition area (HATA) (Figure S1B). For the purpose of the present work, we considered the volumes of the hippocampal body, head, and tail, as well as the whole hippocampal volume.

For the thalamic segmentation, the volume of 25 individual thalamic nuclei was calculated for each side. The nuclei were clustered into six groups according to Iglesias et al.²⁵ as follows: (i) the anteroventral nuclei in the

anterior group; (ii) the laterodorsal and lateral posterior nuclei in the lateral group; (iii) the ventral anterior, ventral anterior magnocellular, ventral lateral anterior, ventral lateral posterior, ventromedial, and ventral posterolateral nuclei in the ventral group; (iv) the central medial, central lateral, paracentral, centromedian, and parafascicular nuclei in the intralaminar group; (v) the paratenial, medial ventral, mediodorsal medial magnocellular, and mediodorsal lateral parvocellular nuclei in the medial group; (vi) and the lateral geniculate, medial geniculate, suprageniculate, pulvinar anterior, pulvinar inferior, pulvinar lateral, and pulvinar medial nuclei in the posterior group (Figure S1C).

Finally, the brainstem was segmented into four regions: medulla, pons, midbrain, and superior cerebellar peduncle (Figure S1D).

Surface-based statistical analyses

After testing for the normality distribution of the data with Shapiro–Wilks test, one-way ANOVAs and chi-squared tests were used to assess differences in demographic and clinical variables among groups and between the patients' groups, and the control group. All subcortical volumes, their sub-parcellations, and the clustered complexes and groups were converted in *z*-scored based on the mean and the standard deviation (SD) of the control population. To account for the side of the EZ, all the subcortical measurements of right-sided patients were flipped to have all the morphometric data of the EZ on the left side. Thus, all morphometric values and results were reported as ipsilateral and contralateral with respect to the EZ. Moreover, to assess for biological brain asymmetry, a pair sample *t*-test was performed for each subcortical volume in the control group.

First, the group differences have been tested for all the morphometric subcortical values using two multivariate analyses of covariance (MANCOVAs): the first, tested the volume differences across all ICA, noICA, and control groups; the second explored the differences only in the TLE subpopulation (i.e., ICA-TLE, noICA-TLE, controls). For each MANCOVA age, gender, and estimated total intracranial volume (eTIV) were included as covariates.¹⁹

Finally, partial correlation analyses were performed between the regions of interest (ROIs) resulting significantly in the MANCOVAs and the clinical variables only in the ICA groups (i.e., all ICA and ICA-TLE). The following ICA-related variables were considered: apnea duration (in sec), desaturation's duration and nadir of desaturation (when present), whether there were group differences in drug-respondent and drug-resistant patients.

The analyses were performed using SPSS software 28 (IBM, Chicago, IL, USA), and statistical significance for

all tests was set at $P < 0.05$. Each analysis has been adjusted for multiple comparisons; P -values were considered significant when surviving a 5% false discovery rate (FDR) correction.²⁸

Results

In the study period, 46 patients met the inclusion criteria: 16 ICA and 30 noICA (Table 1). Among the ICA group, 12 patients were affected by TLE, 3 by frontal lobe epilepsy (FLE), and 1 by insular epilepsy (ILE). Fifteen participants out of the 30 noICA patients had a diagnosis of TLE, while the other 15 of FLE. Statistical analyses did not highlight differences between patient groups and controls in age, sex, distribution, eTIV, age of onset, epilepsy duration, ASMs, and drug responsiveness (Table 1).

Electroclinical data

The detailed electroclinical data of the ICA patients are reported in Table 2. The etiology was either structural (11 out of 16 patients) with a predominance of focal cortical dysplasia (FCDs), or unknown (5 out of 16). Among the ICA patients, we recorded 87 seizures, 42 of which (48.3%) with seizure-related central apnea.

Ten patients had hypoxemia because of ictal apnea, with an oxygen nadir ranging from 89% to 71%. No patient was aware of apnea occurrence. Figure 1 displays the ictal EEG of one representative ICA patient. Clinical details of noICA cohort are summarized in Table S1. In the noICA group, 131 seizures were recorded. Eighteen patients had structural etiology (mainly FCD) while in eight, it was not possible to find the underlying cause of

epilepsy; two patients had an autoimmune cause and two a genetic etiology. The majority of patients (11 out of 16 in the ICA group and 20 out of 30 among the noICA) had drug-resistant epilepsy.¹⁶ At the end of the presurgical evaluation, four ICA patients underwent surgery, but only for one patient (pt#9) the pathology of the amygdala was available and reported as gliosis.

Voxel-based morphometry results

The VBM whole-brain analysis showed an increased gray matter volume of the amygdala ipsilateral to the EZ in the ICA group with respect to noICA patients (MNI coordinates: X: -19.50, Y: -9, Z: -13.50, T maximum = 3.24; number of contiguous voxels: K: 181, $P < 0.190$), while no statically significant differences were observed in both ICA versus controls and noICA versus controls comparison. The sub-analysis in the TLE group demonstrated a greater gray matter volume of the ipsilateral amygdala in the ICA-TLE patients compared with both noICA-TLE group (MNI coordinates: X: -21, Y: -3, Z: -18; T maximum = 4.21; number of contiguous voxels: K: 901, $P < 0.006$) and controls (MNI coordinates: X: -19.5, Y: 3, Z: -27; T maximum = 4.01; number of contiguous voxels: K: 138 $P < 0.234$), while no differences were detected between noICA-TLE and controls (Fig. 2).

Surface-based morphometry results

The statistical analyses of subcortical volumes revealed significant volumetric differences only for the amygdala ipsilateral to the EZ, and its nuclei and complexes. The whole amygdala ipsilateral to the EZ was found to have a greater

Table 1. Clinical and demographic measures of patients (ICA and noICA) and controls. Data are presented in mean (\pm SDs). ASM, antiseizure medication; eTIV, estimated intracranial volume; TLE, temporal lobe epilepsy. # indicate the descriptive analyses and statistics regarding the entire population; * indicate the descriptive analysis and statistics regarding the TLE subgroup; F: ANOVA; X: chi-squared.

	ICA (N = 16)	noICA (N = 30)	Controls (N = 30)	Stat.	P
TLE (y/n)	12/4	15/15			
Age	35.06 (\pm 12.234)#	37.20 (\pm 14.944)#	32.20 (\pm 12.234)	1.041 ^F #	0.358#
	36.17 (\pm 13.037)*	39.47 (\pm 12.755)*		1.737 ^{F*}	0.186*
Gender (F/M)	7/9#	13/17#	15/15	0.312 ^X #	0.856#
	5/7*	7/8*		0.243 ^{X*}	0.886*
eTIV	1.55 ^{E+06} (\pm 1.38 ^{E+05})#	1.58 ^{E+06} (\pm 1.80 ^{E+05})#	1.56 ^{E+06} (\pm 1.41 ^{E+05})	0.186 ^F #	0.831#
	1.54 ^{E+06} (\pm 1.58 ^{E+05})*	1.54 ^{E+06} (\pm 1.54 ^{E+05})*	5)	0.149 ^{F*}	0.862*
Age of onset	21.87 (\pm 14.678)#	22.53 (\pm 13.198)#	–	0.024 ^F #	0.878#
	24 (\pm 13.678)*	27.07 (\pm 13.477)*		0.341 ^{F*}	0.565*
Epilepsy duration	13.36 (\pm 15.028)#	14.72 (\pm 14.660)#	–	0.089 ^F #	0.767#
	12.37 (\pm 15.796)*	12.47 (\pm 13.376)*		0.000 ^{F*}	0.987*
ASM	2.50 (\pm 1.506)#	2.30 (\pm 1.317)#	–	0.218 ^F #	0.643#
	2.42 (\pm 1.240)*	1.60 (\pm 0.986)*		3.643 ^{F*}	0.068*
Drug-respondent (y/n)	15/11#	10/20#	–	0.021 ^X #	0.886#
	4/8*	8/7*		1.080 ^{X*}	0.299*

Table 2. Electroclinical data in the ICA population. Age is expressed in years. M, male; F, female; L, left; R, right; B=bilateral; TLE, temporal lobe epilepsy; FLE, frontal lobe epilepsy; ILE, insular lobe epilepsy; P, parietal; FCD, focal cortical dysplasia; HS, hippocampal sclerosis; LEAT, long-term epilepsy associated tumors; MCD, malformation of cortical development; DR, drug resistance; ASM, antiseizure medications; W, wakefulness. Apnea duration is expressed in seconds, if more than one apnea is recorded, the average length is displayed (\pm SD). Oxygen desaturation is expressed in %. (*): histological report described an amygdala gliosis beyond the FCD in the temporal pole; (**): the detail histology reports a glioneural lesion IDH1R132 wild type. #: follow-up have been reported at 12 months from surgery according to Engel 1993.³⁹

PtID/ age/sex	Side/ epilepsy syndrome	Suspected etiology	Epilepsy duration (years)	No. ASM/ DR	Seizure frequency	Seizure occurrence	Surgery/ histology	Follow- up [#]	No. seizures with ICA/no. of recorded seizures	Apnea duration (mean \pm SD)	Oxygen desaturation (Nadir %)
1/32/ F	L/TLE	Unknown	7	1/no	>1/month	W/NREM	No	N/A	3/3	71.7 (\pm 10.7)	Yes (74%)
2/32/M	R/TLE	FCD	9	1/no	<1/month	W/NREM	Yes/FCD la	la	5/9	25.5 (\pm 23.4)	No
3/25/F	L/TLE	Unknown	10	3/yes	<1/month	W	No	N/A	1/1	16	Yes (89%)
4/51/M	R/TLE	B-P calcifications	43	3/yes	<1/month	NREM	No	N/A	1/1	13	Yes (87%)
5/20/ M	L/TLE	Encephalocele	1	3/yes	>1/month	W	Yes/ gliosis	lb	2/2	31 (\pm 12.73)	Yes (76%)
6/55/F	L/TLE	HS	13	4/yes	>1/week	W	No	N/A	3/4	46.7 (\pm 47.2)	Yes (85%)
7/38/M	L/TLE	FCD	0.5	2/yes	>1/week	W	Yes/ FCDlb*	la	1/1	11	No
8/41/F	R/TLE	FCD	10	3/yes	>1/week	NREM	No	N/A	1/1	30	No
9/50/M	L/TLE	Unknown	2	2/no	>1/week	W/NREM	No	N/A	10/14	37.7 (\pm 44.3)	Yes (87%)
10/21/M	R/TLE	Tumor (parieto- temporal LEAT)	4	3/yes	>1/month	W	Yes/ LEAT**	la	1/1	20	Yes (83%)
11/49/M	L/TLE	MCD	47	4/yes	>1/week	W	No	N/A	1/2	57	Yes (72%)
12/20/F	L/TLE	FCD	2	0/no	<1/month	W	No	N/A	1/1	23	No
13/42/M	R/TLE	Unknown	0.25	1/yes	>1/month	NREM	No	N/A	5/14	20.4 (\pm 20.4)	Yes (80%)
14/43/M	L/TLE	FCD	34	6/yes	>1/week	NREM	No	N/A	2/28	6.5 (\pm 2.8)	No
15/22/F	L/TLE	FCD	19	3/yes	>1/week	NREM	No	N/A	4/4	31.5 (\pm 2.6)	Yes (71%)
16/20/F	R/TLE	Unknown	12	1/yes	>1/month	W	No	N/A	1/1	12	No

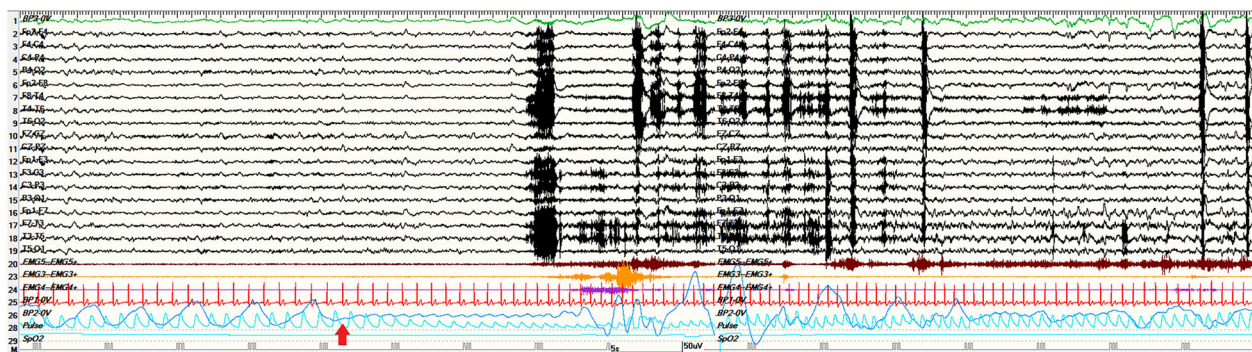


Figure 1. A 2-min view of a left temporal seizure occurring during N2 sleep in a representative ICA patient (pt#9). ICA onset is indicated by the red arrow and precedes the appearance of the electrographic discharge over the left fronto-temporal regions. No hypoxemia was recorded during this seizure. Red channel: EKG; light blue channel: pulse-oxymetry; blue channel: thoracoabdominal respirogram.

volume in ICA versus controls and ICA versus noICA, specifically the BLA (Table 3, Figs. 3 and 4A). The sub-analysis of single amygdalar nuclei showed an increase in the volume of the lateral nucleus in the comparison ICA versus

controls (Table 3 and Fig. 3). The other amygdala nuclei did not show any differences in volume in ICA versus other populations (Table S2) and similarly, no significant differences were noted in the comparison between noICA and

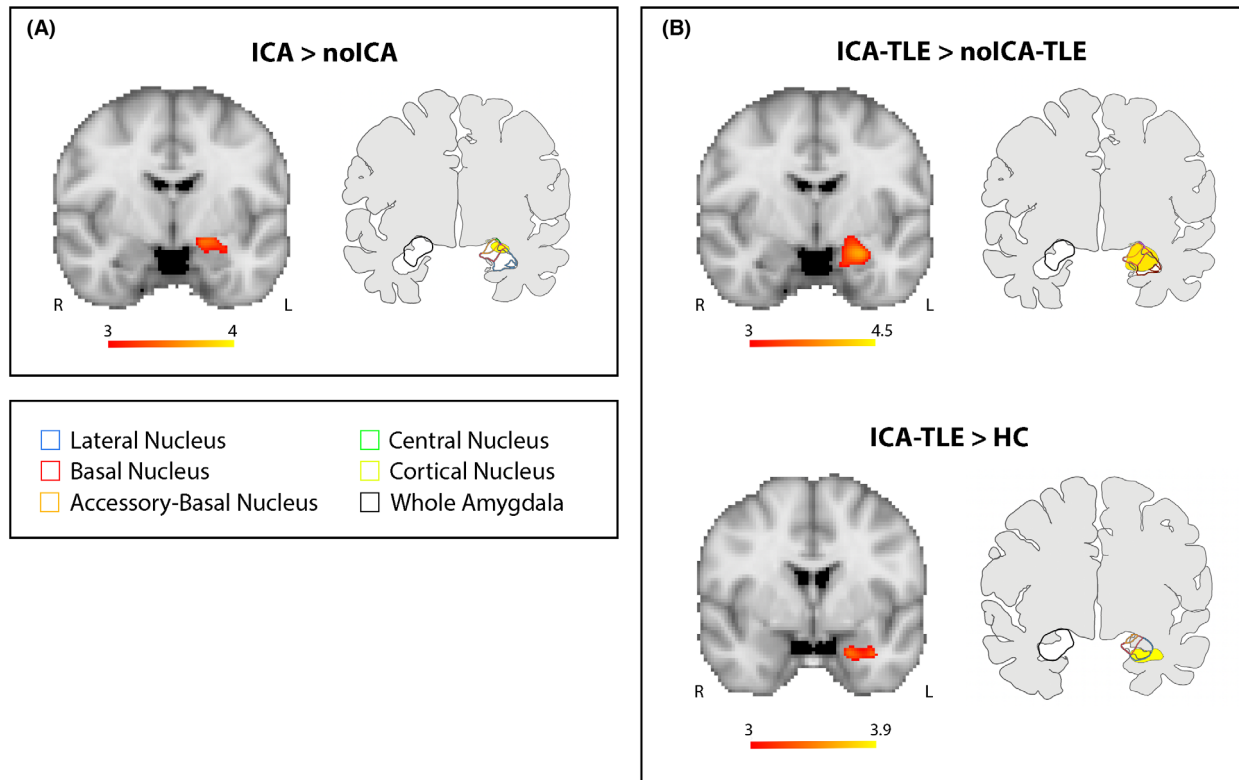
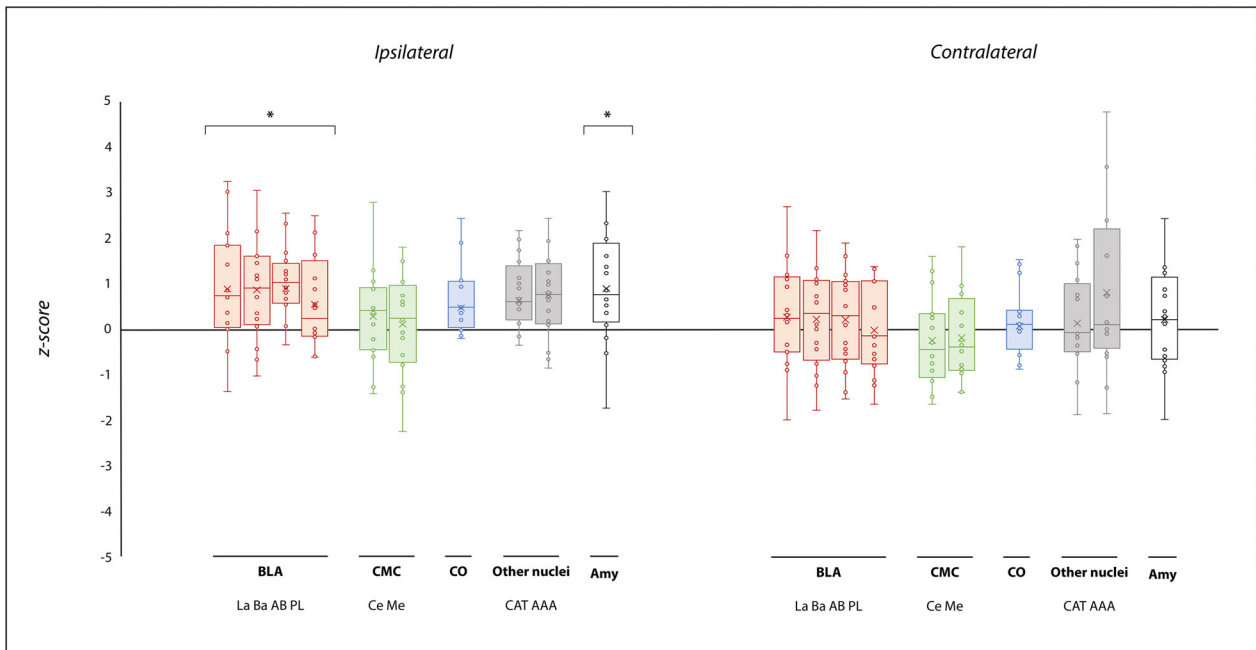


Figure 2. Voxel-based morphometry (VBM) results. Panel (A) VBM analysis looking for gray matter volume increase in ICA compared to noICA patients. Panel (B) VBM analysis exploring gray matter volume increases in ICA-TLE compared to noICA-TLE patients (upper images) and ICA-TLE compared to HC (lower images). For each Panel, left images show significant amygdala enlargement on the left side, ipsilateral to the EZ (details are explained in the methods section). Results are displayed on the coronal Montreal Neurological Institute (MNI) template image (MNI152-T1-2 mm). Color bar reflects T scores. Right images of each panel display the overlap of the VBM results and the amygdala subnuclei segmentation as provided by Saygin et al.²² R = right; L = left.

Table 3. Significant structural morphometric comparisons of ipsilateral amygdala complexes and subnuclei among patient groups and controls. Data are presented in mean(\pm SDs). TLE, temporal lobe epilepsy; BLA, basolateral complex; #: indicate the descriptive analyses and statistics regarding the entire population; *: indicate the descriptive analysis and statistics regarding the TLE subgroup only; °: *P*-values from pairwise comparison analysis were adjusted using FDR (false discovery rate) correction.

Structure	ICA	noICA	Controls	<i>F</i>	<i>P</i>	Pairwise comparisons°
Whole amygdala	1987.231 (\pm 214.919)#	1863.597 (\pm 292.128)#	1800.712 (\pm 183.124)#	5.383#	0.007#	ICA > HC: <i>P</i> = 0.043#; ICA > noICA: <i>P</i> = 0.038
	2016.651 (\pm 231.994)*	1846.685 (\pm 338.526)*	1800.712 (\pm 183.124)*	5.658*	0.006*	#ICA-TLE > HC: <i>P</i> = 0.022*
BLA	1611.857 (\pm 178.427)#	1511.947 (\pm 232.534)#	1452.557 (\pm 152.766)#	5.121#	0.008#	ICA > HC: <i>P</i> = 0.026#; ICA > noICA: <i>P</i> = 0.034#
	1640.033 (\pm 192.793)*	1497.260 (\pm 267.605)*	1452.557 (\pm 152.766)*	6.742*	0.003*	ICA-TLE > HC: <i>P</i> = 0.005*; ICA-TLE > noICA-TLE: <i>P</i> = 0.035*
Lateral	743.436 (\pm 91.861)#	695.239 (\pm 98.912)#	668.163 (\pm 76.014)#	6.160#	0.003#	ICA > HC: <i>P</i> = 0.037#
	760.645 (\pm 99.570)*	688.131 (\pm 109.486)*	668.163 (\pm 76.014)*	8.045*	0.001*	ICA-TLE > HC: <i>P</i> = 0.006*
Basal	516.310 (\pm 60.513)*	470.823 (\pm 92.370)*	457.621 (\pm 49.988)*	5.446*	0.007*	ICA-TLE > HC: <i>P</i> = 0.017*

(A) ICA



(B) noICA

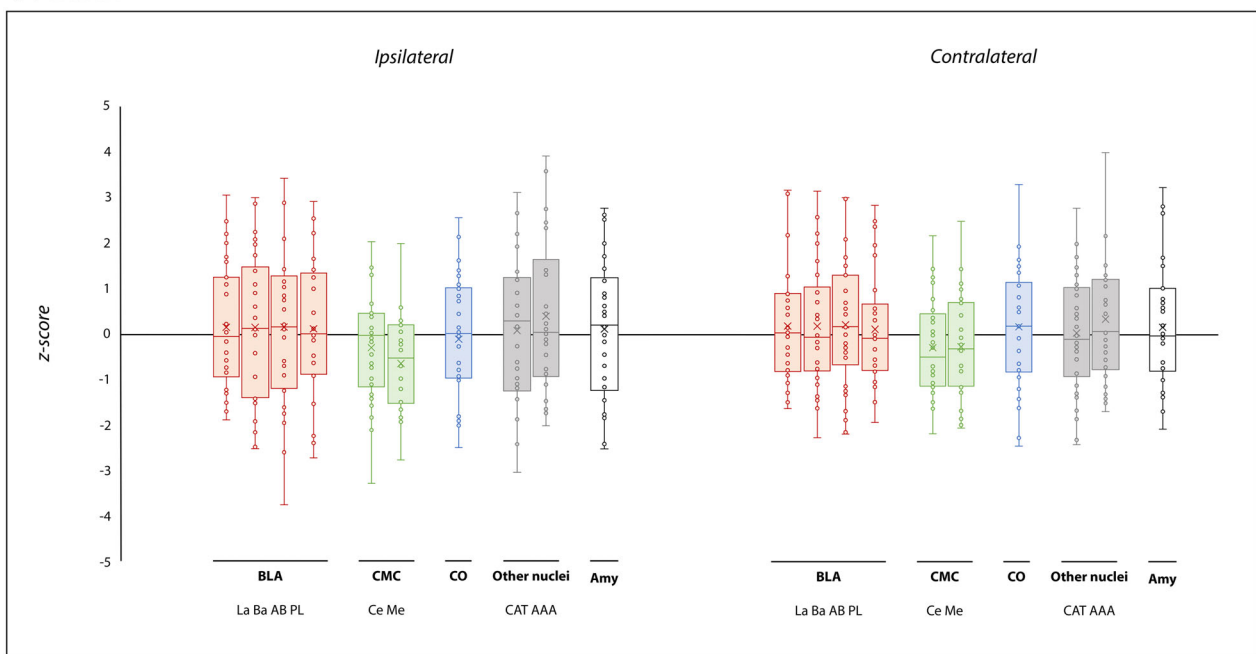


Figure 3. Amygdalar subnuclei comparisons between ICA and noICA groups and controls. Box-and-whisker plots of volumes of amygdalar structures ipsilateral and contralateral to the EZ in ICA (A) and noICA patients (B) standardized relatively to controls. The boxes' central horizontal line marks the median, and the upper and lower edges (the hinges) mark the 25th and 75th percentiles (the central 50% of the values fall within the box). The "x" in the middle of each box marks the mean volume for each nucleus. The open circles represent each patient. The black line on the 0 value designates the mean volume of controls. Finally, the "*" on the boxes indicates the significant results (pFDR < 0.05) from the comparison between patient groups and controls. La, lateral nucleus; Ba, basal nucleus; AB, accessory basal nucleus; PL, paralamina nucleus; Ce, central nucleus; Me, medial nucleus; Co, cortical nucleus; AAA, anterior amygdaloid area; CAT, corticoamygdaloid transition area; BLA, basolateral amygdala; CMC, central-medial complex; CO, cortical complex; Amy, whole amygdala volume.

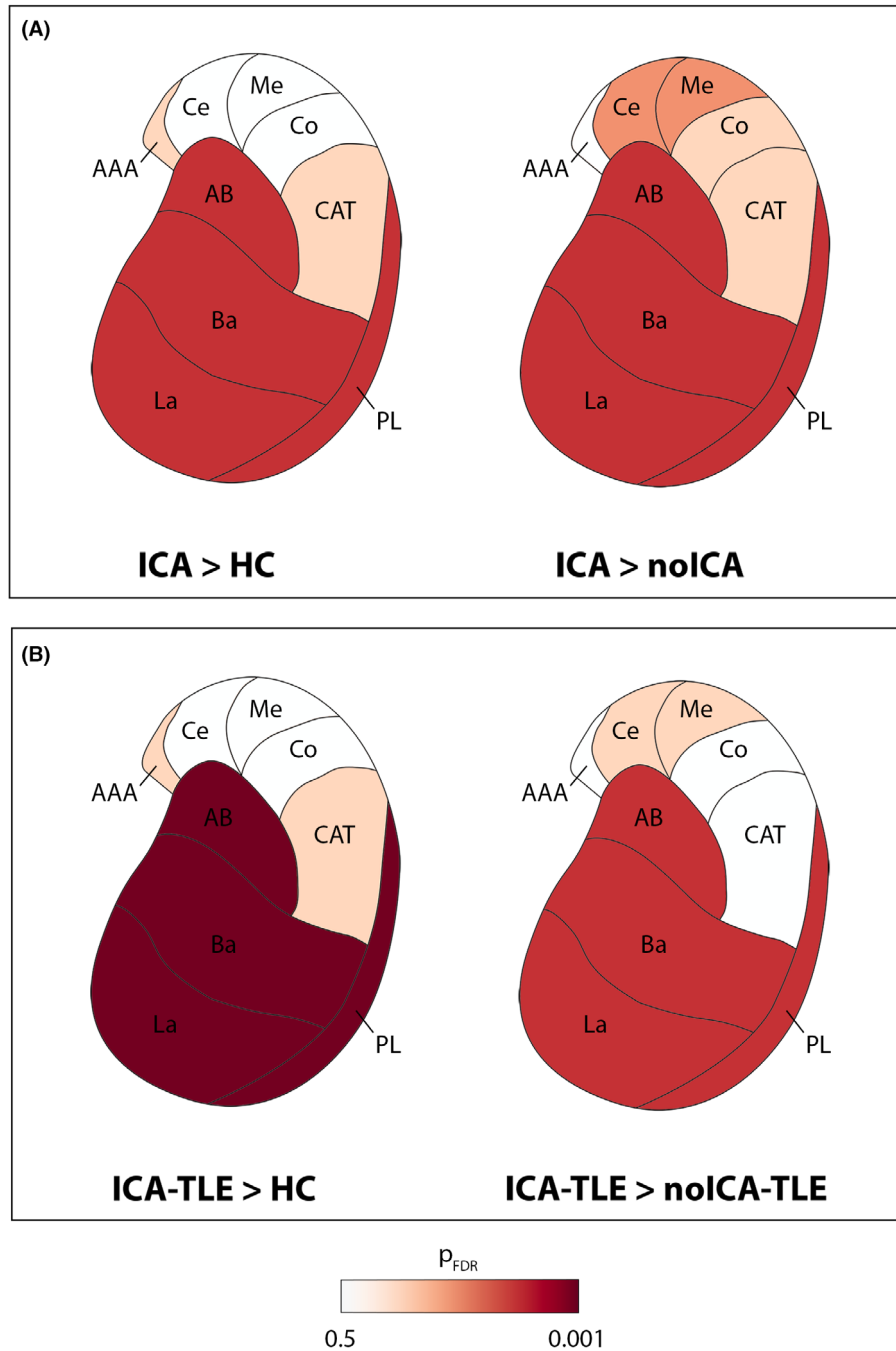


Figure 4. Amygdalar subnuclei comparisons between ICA, noICA, and controls in the whole population and in TLE subgroups. The comparisons between ICA and the other groups (i.e., controls and noICA) are represented using FDR adjusted P -value. Only the amygdala ipsilateral to the EZ is presented. Panel (A) shows the comparison between ICA patients versus controls (left image) and noICA (right image). Panel (B) shows the comparison among the subgroups of ICA-TLE compared to controls (left image), and noICA-TLE (right image). La, lateral nucleus; Ba, basal nucleus; AB, accessory basal nucleus; PL, paralaminar nucleus; Ce, central nucleus; Me, medial nucleus; Co, cortical nucleus; AAA, anterior amygdaloid area; CAT, corticoamygdaloid transition area. See text for details.

controls for any amygdala nucleus (Table S2, Fig. 3). When focusing on TLE patients, the ipsilateral whole amygdala volume was greater for the ICA-TLE group compared to

controls, with the BLA appearing to be greater in volume (Table 3 and Fig. 4B). Moreover, the ICA-TLE patients compared to the noICA group, showed a larger ipsilateral

BLA complex (Table 3 and Fig. 4B). Notably, no differences were found when comparing noICA-TLE patients versus healthy controls. No other statistically relevant modifications were observed for the other subcortical structures including hippocampal, thalamic, and brainstem subfields (Tables S3–S6).

Statistical correlation between ICA-related variables and amygdala volumes did not show any significant association.

Discussion

This study provides evidence that subtle structural volume changes can be found in patients presenting with focal seizures and ICA by means of advanced neuroimaging techniques. ICA is a quite frequent ictal phenomenon, especially, but not exclusively,⁵ among patients with focal epilepsy. Indeed, the incidence of ictal autonomic manifestations and ictal respiratory changes is considered to be higher in temporal lobe seizures.^{1,5,29} This study offers a specific insight on the physiopathological mechanisms of ictal central apnea, which is also regarded as a possible risk factor for SUDEP.^{2,30}

ICA and the basolateral complex

Previous invasive neurophysiological studies^{12–14} reported that the direct electrical stimulation of the amygdala was sufficient to induce a transient respiratory arrest, both in relation to ictal activity and as a physiological response. Within the amygdala, the implicated nuclei seem to be the basal, lateral, and central. Specifically, one study¹² identified the lateral and basal nuclei to be the most implicated in generating the apneic response, while other authors³¹ pointed out that only the direct stimulation of the central nucleus could lead to central apnea. Later, Lacuey *et al.*¹³ found that low- and high-frequency stimulation of basal and central nuclei induced apnea, while only high-frequency stimulation of the lateral nucleus was needed to obtain the apneic phenomenon.

According to this evidence, our advanced neuroimaging findings showed that the whole amygdala ipsilateral to the EZ is increased in volume in patients with ICA, with the BLA being the most involved when considering the amygdala subnuclei. This volumetric increase confirms and expands previous suggestions regarding the involvement of the amygdala and specifically of the BLA in the epileptic network of patients with ictal central apnea.

In the ICA group, the BLA was significantly greater in volume in comparison to both noICA patients and healthy controls. This observation could lead to the hypothesis that the BLA enlargement on advanced neuroimaging might be a biomarker for ICA occurrence in patients with focal epilepsy. This finding was supported

by even stronger statistical significance when considering only the TLE patients. Thus, the ictal central apneic phenomenon may be reasonably a distinctive hallmark of temporal lobe epilepsy rather than extra-temporal seizures, as already reported.^{1,5,29} Nevertheless, we already showed that even an ictal discharge that originates from extra-temporal cortical areas may secondarily involve the temporal regions causing the ictal respiratory arrest.⁵

Of note, considering the presence of hippocampal sclerosis, only one ICA-TLE patient presented with this radiological finding, while this was evident in five noICA-TLE patients. As already reported in the literature, it was demonstrated that HS was significantly associated with volumetric reduction of the ipsilateral amygdala and, in particular, of the BLA.²⁷ It could be argued that amygdalar atrophy could partially explain the volumetric differences between these two groups. However, the comparison against the healthy control group corroborates our main hypothesis that the volumetric changes may be more likely related to the apnea occurrence. We could also speculate that HS could be somehow protective against ictal respiratory arrest, but further evidence is warranted.

As for the anatomic-physiological aspects, the BLA is constituted of the lateral nucleus, the basal nucleus, the accessory basal nucleus, and the paralaminar nucleus and comprises the majority of the total amygdala volume in humans.³² This complex of the amygdala receives strong sensory input from multiple cortical and thalamic sources which terminate primarily in the lateral nucleus, and has reciprocal interactions with the hippocampal formation, including the entorhinal cortex, perirhinal cortex, and parahippocampal cortex.^{33,34} The BLA is composed of neurons that resemble the pyramidal neurons of the cortex, leading to the hypothesis that for some TLE cases the primary epileptogenic focus in mesial TLE might be the amygdala itself and, specifically, the BLA.^{13,34} While the lateral nucleus does not directly project to the brainstem, it might influence the apneic response through intrinsic connections to amygdala nuclei or through hippocampal and thalamic projections.

The amygdala increased volume and SUDEP risk

Previous studies investigated the cortical and subcortical morphometric modifications in SUDEP patients and in patients with epilepsy considered to be at higher risk for SUDEP.^{35–37} Different morphometric alterations were found in terms of cortical thickness and volume of brain structures, in the direction of tissue gain as well as atrophy. Specifically, in a previous study, the right amygdala appeared to have an increased volume in cases of SUDEP and those at high risk compared with low-risk and healthy

controls.³⁵ Other authors observed a volumetric increase of the amygdala bilaterally in SUDEP patients versus healthy controls and of the right amygdala in high-risk patients compared to controls.³⁶ It is well known that peri-ictal respiratory impairment represents a risk factor for SUDEP. Our data provide an “imaging” link between ICA and SUDEP and confirm the key role of the amygdala in the pathophysiology of both phenomena. The hypertrophy of the amygdala might be due to structural rearrangements, possibly secondary to the long-standing epileptic activity.³⁸ As a consequence, the tissue gain of the amygdala might correspond to a gain of function, therefore leading to more chances that ictal apnea/SUDEP to occur.

Study limitations

Despite our novel findings, this study presents some limitations. First, the number of participants is limited which could be due to the relatively short study-period and to strict inclusion criteria for patient recruitment. In particular, the number of extra-TLE patients with ICA is limited, thus preventing us from performing a thorough electro-clinical and imaging characterization of this population. In this scenario, our findings of a greater amygdala volumes in ICA-TLE patients need to be verified by further studies including a higher number of extra-TLE patients. Second, the absence of correlation with clinical variables needs to be interpreted with caution given the small study population. Of note, however, this finding could be of interest to better understand the pathophysiology of apnea phenomena. The amygdalar volume increases can represent indeed a biomarker *per se* independently of any other clinical factor and, in particular, of apnea severity. Overall, our data support the need of larger multicenter studies to overcome these limitations and provide further evidence supporting these novel results.

Author Contributions

Elisa Micalizzi: conceptualization (equal); data curation (equal); writing—original draft (lead); formal analysis (supporting); writing—review and editing (equal). **Alice Ballerini:** data curation (equal); methodology (equal); formal analysis (lead); writing—original draft (supporting); writing—review and editing (equal). **Giada Giovannini:** investigation (supporting); writing—review and editing (supporting). **Maria C. Cioclu:** investigation (supporting); writing—review and editing (supporting). **Simona Scolastico:** writing—review and editing (supporting). **Matteo Pugnaghi:** investigation (supporting); writing—review and editing (supporting). **Niccolò Orlandi:** investigation (supporting); writing—review and editing (supporting). **Marcella Malagoli:** investigation

(supporting); writing—review and editing (supporting). **Maurilio Genovese:** investigation (supporting); writing—review and editing (supporting). **Alessandra Todeschini:** investigation (supporting); writing—review and editing (supporting). **Leandra Giunta:** investigation (supporting); writing—review and editing (supporting). **Flavio Villani:** writing—review and editing (equal). **Stefano Meletti:** conceptualization (equal); writing—review and editing (equal). **Anna E. Vaudano:** conceptualization (equal); methodology (lead); writing—review and editing (equal).

Acknowledgments

This study was supported by a grant “Dipartimenti di eccellenza 2018–2022,” MIUR, Italy, to the Department of Biomedical, Metabolic and Neural Sciences and by a grant “Ricerca Finalizzata,” project code NET-2013-02355313, Ministry of Health to the Azienda Ospedaliera-Universitaria di Modena “Centro hub chirurgia epilessia” (DGR 1172/18).

Conflict of interest

E. Micalizzi has served as a paid consultant for Angelini Pharma. F. Villani has served as a paid consultant and received support from Angelini Pharma, UCB Pharma, EISAI, Lusofarmaco, Jazz Pharma, Bial.S. Meletti has served as a paid consultant and received support from the Ministry of Health (MOH), UCB, GW, Jazz pharmaceuticals and EISAI. A.E. Vaudano has served as a paid consultant for Angelini Pharma. The other authors report no conflict of interest.

Standard protocol approvals, registrations, and patient consents

The study was approved by the local ethical committee of Area Vasta Emilia Nord (NET-2013-02355313 N.322/15 and 679/2022/SPER/UNIMO). Patients and controls gave written informed consent for the use of their clinical records in this study. The study was conducted in accordance with the World Medical Association Declaration of Helsinki.

Data availability statement

Anonymized data not published within this article will be made available by request from any qualified investigator.

References

1. Lacuey N, Zonjy B, Hampson JP, et al. The incidence and significance of periictal apnea in epileptic seizures. *Epilepsia*. 2018;59(3):573-582. doi:10.1111/epi.14006

2. Vilella L, Lacuey N, Hampson JP, et al. Incidence, recurrence, and risk factors for peri-ictal central apnea and sudden unexpected death in epilepsy. *Front Neurol*. 2019;10:166. doi:[10.3389/fneur.2019.00166](https://doi.org/10.3389/fneur.2019.00166)
3. Ryvlin P, Nashef L, Lhatoo SD, et al. Incidence and mechanisms of cardiorespiratory arrests in epilepsy monitoring units (MORTEMUS): a retrospective study. *Lancet Neurol*. 2013;12(10):966-977. doi:[10.1016/S1474-4422\(13\)70214-X](https://doi.org/10.1016/S1474-4422(13)70214-X)
4. Micalizzi E, Vaudano AE, Giovannini G, Turchi G, Giunta L, Meletti S. Case report: ictal central apnea as first and overlooked symptom in temporal lobe seizures. *Front Neurol*. 2021;12:753860. doi:[10.3389/fneur.2021.753860](https://doi.org/10.3389/fneur.2021.753860)
5. Micalizzi E, Vaudano AE, Ballerini A, et al. Ictal apnea: a prospective monocentric study in patients with epilepsy. *Eur J Neurol*. 2022;29(12):3701-3710. doi:[10.1111/ene.15547](https://doi.org/10.1111/ene.15547)
6. Bailey P, Sweet WH. Effects on respiration, blood pressure and gastric motility of stimulation of orbital surface of frontal lobe. *J Neurophysiol*. 1940;3(3):276-281. doi:[10.1152/jn.1940.3.3.276](https://doi.org/10.1152/jn.1940.3.3.276)
7. Smith WK. The functional significance of the rostral cingular cortex as revealed by its responses to electrical excitation. *J Neurophysiol*. 1945;8(4):241-255. doi:[10.1152/jn.1945.8.4.241](https://doi.org/10.1152/jn.1945.8.4.241)
8. Kaada BR, Pribram KH, Epstein JA. Respiratory and vascular responses in monkeys from temporal pole, insula, orbital surface and cingulate gyrus: a preliminary report. *J Neurophysiol*. 1949;12(5):347-356. doi:[10.1152/jn.1949.12.5.347](https://doi.org/10.1152/jn.1949.12.5.347)
9. Hoffman BL, Rasmussen T. Stimulation studies of insular cortex of macaca mulatta. *J Neurophysiol*. 1953;16(4):343-351. doi:[10.1152/jn.1953.16.4.343](https://doi.org/10.1152/jn.1953.16.4.343)
10. Penfield W, Jasper HH. Epilepsy and the functional anatomy of the human brain. 1st ed. Little, Brown; 1954.
11. Nelson DA, Ray CD. Respiratory arrest from seizure discharges in limbic system: report of cases. *Arch Neurol*. 1968;19(2):199-207. doi:[10.1001/archneur.1968.00480020085008](https://doi.org/10.1001/archneur.1968.00480020085008)
12. Dlouhy BJ, Gehlbach BK, Kreple CJ, et al. Breathing inhibited when seizures spread to the amygdala and upon amygdala stimulation. *J Neurosci*. 2015;35(28):10281-10289. doi:[10.1523/JNEUROSCI.0888-15.2015](https://doi.org/10.1523/JNEUROSCI.0888-15.2015)
13. Lacuey N, Hampson JP, Harper RM, Miller JP, Lhatoo S. Limbic and paralimbic structures driving ictal central apnea. *Neurology*. 2019;92(7):e655-e669. doi:[10.1212/WNL.0000000000006920](https://doi.org/10.1212/WNL.0000000000006920)
14. Nobis WP, González Otárula KA, Templer JW, et al. The effect of seizure spread to the amygdala on respiration and onset of ictal central apnea. *J Neurosurg*. 2020;132(5):1313-1323. doi:[10.3171/2019.1.JNS183157](https://doi.org/10.3171/2019.1.JNS183157)
15. Kanth K, Park K, Seyal M. Severity of peri-ictal respiratory dysfunction with epilepsy duration and patient age at epilepsy onset. *Front Neurol*. 2020;11:618841. doi:[10.3389/fneur.2020.618841](https://doi.org/10.3389/fneur.2020.618841)
16. Kwan P, Arzimanoglou A, Berg AT, et al. Definition of drug resistant epilepsy: consensus proposal by the ad hoc Task Force of the ILAE commission on therapeutic strategies. *Epilepsia*. 2010;51(6):1069-1077. doi:[10.1111/j.1528-1167.2009.02397.x](https://doi.org/10.1111/j.1528-1167.2009.02397.x)
17. Bernasconi A, Cendes F, Theodore WH, et al. Recommendations for the use of structural magnetic resonance imaging in the care of patients with epilepsy: a consensus report from the International League Against Epilepsy Neuroimaging Task Force. *Epilepsia*. 2019;60(6):1054-1068. doi:[10.1111/epi.15612](https://doi.org/10.1111/epi.15612)
18. Vaudano AE, Ballerini A, Zucchini F, et al. Impact of an optimized epilepsy surgery imaging protocol for focal epilepsy: a monocentric prospective study. *Epileptic Disord*. 2023;25(1):45-56. doi:[10.1002/epd2.20050](https://doi.org/10.1002/epd2.20050)
19. Backhausen LL, Herting MM, Buse J, Roessner V, Smolka MN, Vetter NC. Quality control of structural MRI images applied using FreeSurfer—A hands-on workflow to rate motion artifacts. *Front Neurosci*. 2016;10:558. doi:[10.3389/fnins.2016.00558](https://doi.org/10.3389/fnins.2016.00558)
20. Whelan CD, Altmann A, Botía JA, et al. Structural brain abnormalities in the common epilepsies assessed in a worldwide ENIGMA study. *Brain*. 2018;141(2):391-408. doi:[10.1093/brain/awx341](https://doi.org/10.1093/brain/awx341)
21. Larivière S, Rodríguez-Cruces R, Royer J, et al. Network-based atrophy modeling in the common epilepsies: a worldwide ENIGMA study. *Sci Adv*. 2020;6(47):eabc6457. doi:[10.1126/sciadv.abc6457](https://doi.org/10.1126/sciadv.abc6457)
22. Park BY, Lariviere S, Rodríguez-Cruces R, et al. Topographic divergence of atypical cortical asymmetry and regional atrophy patterns in temporal lobe epilepsy: a worldwide Enigma study. *Brain*. 2022;145:1285-1298. doi:[10.1101/2021.04.30.442117](https://doi.org/10.1101/2021.04.30.442117)
23. Saygin ZM, Kliemann D, Iglesias JE, et al. High-resolution magnetic resonance imaging reveals nuclei of the human amygdala: manual segmentation to automatic atlas. *Neuroimage*. 2017;155:370-382. doi:[10.1016/j.neuroimage.2017.04.046](https://doi.org/10.1016/j.neuroimage.2017.04.046)
24. Iglesias JE, Augustinack JC, Nguyen K, et al. A computational atlas of the hippocampal formation using ex vivo, ultra-high resolution MRI: application to adaptive segmentation of in vivo MRI. *Neuroimage*. 2015;115:117-137. doi:[10.1016/j.neuroimage.2015.04.042](https://doi.org/10.1016/j.neuroimage.2015.04.042)
25. Iglesias JE, Insausti R, Lerma-Usabiaga G, Bocchetta M, Van Leemput K, Greve DN, Van der Kouwe A, Fischl B, Caballero-Gaudes C, Paz-Alonso PM; Alzheimer's Disease Neuroimaging Initiative. A probabilistic atlas of the human thalamic nuclei combining ex vivo MRI and histology. *Neuroimage*. 2018;183:314-26. Accessed March 18, 2022. <http://arxiv.org/abs/1806.08634>
26. Iglesias JE, Van Leemput K, Bhatt P, et al. Bayesian segmentation of brainstem structures in MRI. *Neuroimage*. 2015;113:184-195. doi:[10.1016/j.neuroimage.2015.02.065](https://doi.org/10.1016/j.neuroimage.2015.02.065)

27. Ballerini A, Tondelli M, Talami F, et al. Amygdala subnuclear volumes in temporal lobe epilepsy with hippocampal sclerosis and in non-lesional patients. *Brain Commun.* 2022;4(5):fcac225. doi:10.1093/braincomms/fcac225
28. Benjamini Y, Hochberg Y. Controlling the false discovery rate: a practical and powerful approach to multiple testing. *J R Stat Soc Ser B Methodol.* 1995;57(1):289-300. doi:10.1111/j.2517-6161.1995.tb02031.x
29. Tio E, Culler GW, Bachman EM, Schuele S. Ictal central apneas in temporal lobe epilepsies. *Epilepsy Behav.* 2020;112:107434. doi:10.1016/j.yebeh.2020.107434
30. Schuele SU, Afshari M, Afshari ZS, et al. Ictal central apnea as a predictor for sudden unexpected death in epilepsy. *Epilepsy Behav.* 2011;22(2):401-403. doi:10.1016/j.yebeh.2011.06.036
31. Nobis WP, Schuele S, Templer JW, et al. Amygdala-stimulation-induced apnea is attention and nasal-breathing dependent: amygdala stimulation and breathing. *Ann Neurol.* 2018;83(3):460-471. doi:10.1002/ana.25178
32. LeDoux J. The amygdala. *Curr Biol.* 2007;17(20):R868-R874. doi:10.1016/j.cub.2007.08.005
33. Aggleton JP, Burton MJ, Passingham RE. Cortical and subcortical afferents to the amygdala of the rhesus monkey (*Macaca mulatta*). *Brain Res.* 1980;190(2):347-368. doi:10.1016/0006-8993(80)90279-6
34. Benarroch EE. The amygdala: functional organization and involvement in neurologic disorders. *Neurology.* 2015;84(3):313-324. doi:10.1212/WNL.0000000000001171
35. Wandschneider B, Koepp M, Scott C, et al. Structural imaging biomarkers of sudden unexpected death in epilepsy. *Brain.* 2015;138(10):2907-2919. doi:10.1093/brain/awv233
36. Allen LA, Vos SB, Kumar R, et al. Cerebellar, limbic and midbrain volume alterations in sudden unexpected death in epilepsy (SUDEP). *Epilepsia.* 2019;60(4):718-729. doi:10.1111/epi.14689
37. Allen LA, Harper RM, Lhatoo S, Lemieux L, Diehl B. Neuroimaging of sudden unexpected death in epilepsy (SUDEP): insights from structural and resting-state functional MRI studies. *Front Neurol.* 2019;10:185. doi:10.3389/fneur.2019.00185
38. Minami N, Morino M, Uda T, et al. Surgery for amygdala enlargement with mesial temporal lobe epilepsy: pathological findings and seizure outcome. *J Neurol Neurosurg Psychiatry.* 2015;86(8):887-894. doi:10.1136/jnnp-2014-308383
39. Engel J. *Surgical treatment of epilepsies.* 2nd ed. Raven Press; 1993.

Supporting Information

Additional supporting information may be found online in the Supporting Information section at the end of the article.

Figure S1. Segmentation and sub-segmentation algorithms of subcortical structures.

Table S1. Clinical details of noICA cohort.

Table S2. Non-significant structural morphometric comparison of bilateral amygdala subnuclei among patient groups and controls.

Table S3. Morphometric comparison of lateral ventriculi, basal ganglia, and cerebellum among patient groups and controls.

Table S4. Morphometric comparison of bilateral hippocampi's subfields among patient groups and controls.

Table S5. Morphometric comparison of bilateral thalamic subnuclei among patient groups and controls.

Table S6. Morphometric comparisons of brainstem substructures among patient groups and controls.

Appendix: ICA is a frequent clinical correlate of focal seizures, particularly involving the temporal lobe and limbic network. According to the literature, the amygdala appears to play a key role in giving rise to the apneic response. Our findings on neuroimaging data support what has already been demonstrated about the involvement of the basolateral complex ipsilateral to the EZ, also suggesting that the volume increase of this specific amygdalar subregion could be a distinctive hallmark of ICA in patients with epilepsy. The identification of valuable biomarkers of ictal autonomic manifestations is needed for a more accurate stratification of the SUDEP risk.